Structural Damage Detection based on Virtual Element Boundary Measurement

C. Zhang[1, 2, 3], L. Cheng[1, 2*], H. Xu[1, 2] and J. H. Qiu[3]

[1] Department of Mechanical Engineering, The Hong Kong Polytechnic University, Hong Kong

[2]The Hong Kong Polytechnic University Shenzhen Research Institute, Shenzhen 518057, China

[3]The State Key Laboratory of Mechanics and Control of Mechanical Structures,

Nanjing University of Aeronautics and Astronautics, Nanjing 210016, China

Submitted to *Journal of Sound and Vibration*

Abstract

A "weak" formulation of the Pseudo-Excitation (PE) approach was recently proposed for structural damage detection in thin-walled structures. The method was shown to exhibit some appealing features including high noise tolerant ability. However, the method requires very dense displacement field measurement within the inspection region. To tackle the problem, a new damage detection method based on virtual element boundary measurement (VEBM) under the "weak" formulation framework is proposed in this paper. VEBM based "weak" formulation divides the entire structure into several "virtual elements" (VE). By tuning the vibration frequency to the natural frequency of the VE, the "weak" formulation is shown to provide a "region-by-region" detection strategy, allowing reliable damage detections by using only a small number of measurement points at the VE boundaries. The effectiveness of the

* To whom correspondence should be addressed
Email: li.cheng@polyu.edu.hk (Prof. Li CHENG, *Ph.D.*)

proposed method was first validated numerically using a cantilever beam containing a small damage. Influences of various factors such as measurement noise levels and frequency discrepancies between the ideal and the actual elements were discussed. An experiment was carried out through a Laser Doppler Vibrometer (LDV) measurement. Results demonstrated that VEBM method is able to achieve good detection results by using a small number of measurement points, whilst providing enhanced noise tolerant capability against measurement uncertainties.

Keywords: Pseudo-Excitation Approach; Damage Detection; Noise Immunity Capability.

1 Introduction

The safety and reliability of engineering structures cannot be over-emphasized. Along with it is the ever-increasing need for effective and reliable damage detection methods. During the last few decades, a large variety of non-destructive evaluation (NDE) methods, such as ultrasonic C-scan [1], eddy-current [2], thermography [3], laser ultrasonic [4], guided-wave [5] etc., have been developed. Among existing methods, vibration based approach is one of the most studied techniques, due to their relatively low cost and potential to be used for on-line structural health monitoring (SHM) [6-10]. Damage indices based on various vibration parameters such as eigen-frequencies, mode shapes, transfer functions, damping properties or electro-mechanical impedance, were proposed to detect the changes in the structural properties as a result of occurrence of the damage [11-15]. Notably, the "pseudo-excitation" (PE) approach was recently proposed to provide a damage detection framework by evaluating the damage-induced perturbation to the local equation of motion [16-20]. The basic principle of PE method is similar to a local force identification problem [21-23]. Compared with other vibration based methods, PE approach shows its advantages in that it requires no prior knowledge on the baseline signals, overall structural models or boundary conditions and so on. Moreover, since PE approach examines the local equation of motion point-by-point, it can be applied to complex systems comprising various structural components like beams, plates and shells.

The original version of the PE approach leads to a damage location index based on the "strong" formulation in which high-order derivatives of the structural displacement need to be derived. In the case of a beam element, for example, $d^4w(x)/dx^4$ (where $w(x)$ is the flexural displacement of the beam element at the position x), is involved. This high order derivative makes "strong" formulation based PE approach venerable to the measurement noise and

uncertainties. Attempts were made in previous works for enhancing the noise immunity. For example, by exploring the relationship between the density of the measurement point and the accuracy of the finite difference scheme used to calculate the high-order derivatives, it was shown that the noise influence can be partly reduced through a proper selection of the measurement interval [16]. Gaussian wavelet transform has also been used in "strong" formulation to construct a multi-scale PE model for damage identifications [17]. Furthermore, a "weak" formulation was also developed using a continuous gauss smoothing-based detection strategy [20]. As a result of the weighted integration, the noise immunity was shown to be improved from "strong" to "weak" formulation. Despite the effort, the latest "weak" version of the PE technique still cannot completely resolve its bottlenecking problems which mainly exhibit in the following aspects: 1) limited by the "point-to-point" inspection strategy and the need for deriving higher-order derivatives, a large amount of measurement points are still required, making it difficult to implement in practical applications; 2) the use of high order derivative can still not be avoided; and 3) the requirement for the structure parameters, such as modulus of elasticity and density is rather harsh, creating another problem since discrepancies between the ideal and actual structural properties are unavoidable.

To address these problems, a novel "weak" form of the PE approach based on virtual element boundary measurement (VEBM) is proposed in this paper. Different from the previous "weak" formulation that directly integrates the damage location index calculated by "strong" formulation within a small interval, VEBM based "weak" formulation firstly divides the entire structure into several regions, which are referred to as "virtual elements" (VE). According to the parameters of VEs, a suitable weight function is chosen to carry out damage location index integration, leading to the final form of "weak" formulation, which only requires vibration measurement at the boundaries of the VEs. Thus, whilst ensuring an

improved robustness against measurement noise through the weighted integration, VEBM based “weak” formulation further reduces the number of the measurement points significantly.

The outline of the paper is as follows. The principle of the VEBM based “weak” formulation is firstly derived from its “strong” counterpart. Selections of the excitation frequency and the weight function are then discussed. Numerical simulations using a finite element model are then presented to demonstrate the effectiveness of the proposed method in terms of de-noising and damage detection capability. Effects of different noise levels and the unavoidable errors in the excitation frequency selection are also discussed. Finally, an experiment is carried out to validate the proposed method using a beam element containing an artificial damage.

2 PE approach for damage detection

2.1 “Strong” formulation

Figure 1 shows a typical complex system comprising various structural components such as beams, plates and shells. Despite the complexity of the overall structure, the dynamic response of each component (and each point on that component) satisfies a certain well-prescribed relation such as the equation of motion. The basic idea of the PE approach is to examine whether the vibration displacement satisfies the local equation of motion in the healthy condition. Since the inspection philosophy is component specific, the structural part beyond the inspected area, although obviously affects the vibration of the inspected component, but does not affect the way that local equation of motion is satisfied. Thus, PE approach can be applied to a complex system by examining the corresponding local equation of motion component-by-component.

Taking an Euler-Bernoulli beam component with homogeneous isotropic material properties under a flexural harmonic excitation as a simple example, a one-dimensional damage location index DLI(x) quantifying the damage-induced perturbation at the position x can be defined as

$$\mathrm{DLI}(x) = EI\frac{\mathrm{d}^4 w(x)}{\mathrm{d}x^4} - \rho S\omega^2 w(x) \tag{1}$$

where ω is the angular vibration frequency of the steady vibration; E, I, ρ and S are modulus of elasticity, cross-sectional moment of inertia, density of material and cross sectional area in healthy structural situation, which are known parameters before damage detection; $w(x)$ is the steady transverse displacement of the beam, that needs to be measured point-by-point during the damage detection. It should be mentioned that, DLI(x) = 0 indicates the vibration of the structural element, in the absence of the surface loading, irrespective of the boundary condition of the entire structure. Physically, DLI(x) represents the transverse excitation over the local area of the beam element. For a pristine component in the absence of any external excitation, DLI(x) = 0 in the intact region, but different from zero within the damage zone, corresponding to a virtual pseudo-excitation due to the structural damage. More details about the derivation of "strong" formulation in damage zone can be found in [16]. Thus, PE approach can detect the damage location where the sudden change exists in the DLI(x) curve. Considering that DLI(x) is a complex function of damage size and shape, "strong" formulation can hardly detect the damage severity in detail, even though DLI(x) quantitatively identifies the deviation from the local equation of motion of the healthy structure.

Similarly, a two-dimensional PE approach can be derived for a homogeneous isotropic plate component using the thin-plate theory, as

$$\mathrm{DLI}(x, y) = \left[D \cdot \nabla^4 - \rho h\omega^2 \right] w(x, y) \tag{2}$$

where $D = Eh^3/12(1-\nu^2)$ is the flexural rigidity of the plate, h and ν are the thickness and Poisson's ratio of the component, respectively. The operator ∇^4, called the Biharmonic operator, can be written as

$$\nabla^4 = \frac{\partial^4}{\partial x^4} + 2\frac{\partial^4}{\partial x^2 \partial y^2} + \frac{\partial^4}{\partial y^4} \tag{3}$$

Both Eqs. (1) and (2) are derived from an undamped structural model of the bending vibration, which is assumed to dominate the structural motion. Considering that light damping takes significant effect on the vibration mainly in the vicinity of structural resonances, the damping influence on local equation of motion can be ignored when excitation frequency is different from any natural frequencies of the structure. Furthermore, the damage is a discontinuous zone in the structure, especially at the damage edge, the singularity in the local equation of motion induces a sudden change in the damage location index that is used to detect the damage position. Thus, "strong" formulation is still effective when possible other types of vibration and damping are present in the structural vibration.

For implementation of "strong" formulation, the vibration displacement fields $w(x)$ (for beam component) and $w(x, y)$ (for plate component) should be measured point by point. For illustration, the continuous vibration displacement $w(x)$ in a beam component is obtained in discrete form w_i. The discrete DLI_i at measurement point i can be calculated by mean of finite difference, using four adjacent measurement points from i-2 to i+2, as

$$\mathrm{DLI}_i = EI\left(\frac{w_{i-2} - 4w_{i-1} + 6w_i - 4w_{i+1} + w_{i+2}}{d_{\mathrm{m}}^4}\right) - \rho S\omega^2 w_i \tag{4}$$

where d_{m} is the interval of measurement points. To achieve a good approximation of the 4th-order derivative, a small d_{m} should be used, leading to very dense measurement. However, due to the high order finite difference employed in Eq. (4), DLI_i is highly sensitive to

measurement noise which is unavoidable in practical applications. Note that, although PE approach, such formulated, is baseline-free, an accurate estimation of the system parameters such as E, I, ρ and S is a prerequisite. Considering the difficulty in obtaining these parameters accurately in practice, especially under changing working environment, the "strong" formulation based PE approach shows its obvious drawbacks with venerable noise immunity.

2.2 "Weak" formulation

For an Euler-Bernoulli beam component, in order to enhance the noise immunity of the PE approach, a "weak" formulation is established by integrating DLI(x) in an interval [x_c-τ/2, x_c+τ/2] with a weight function $\eta(x)$ as

$$\overline{\mathrm{DLI}}\left(x_c,\tau\right)=\int_{x_c-\tau/2}^{x_c+\tau/2}\left[EI\frac{\mathrm{d}^4w\left(x\right)}{\mathrm{d}x^4}-\rho S\omega^2w\left(x\right)\right]\eta\left(x-x_c\right)\mathrm{d}x \tag{5}$$

where $\overline{\mathrm{DLI}}$ represents the "weak" formulation based damage location index; x_c and τ are the center and width of the interval, respectively. Taking advantage of the weighted integration, $\overline{\mathrm{DLI}}$ quantifies the local equation of motion within the integrative interval instead of at each specific point. It was proven that the measurement noise can be partly suppressed and the signal feature pertaining to the damage can be strengthened using a classic Gaussian weigh function [20].

The physical implication of the "weak" formulation is to examine the structure 'region-by-region'. In doing so, the DLI in "strong" formulation is summed up over the interval that averages the noise. However, the amount of data points required in the measurement is still the same. Furthermore, the high-order derivative still remains which intrinsically arouses inaccuracies due to the measurement noise.

3. VEBM based “weak” formulation

3.1 Damage location index of the VE

The noise from the displacement measurement is magnified in PE approach by the high-order derivatives. For reducing the derivative order of $w(x)$, integration par part is carried out, thus diverting the derivative from actual displacement $w(x)$ to weight function $\eta(x)$ gradually. Eventually, the 4th-order derivative in Eq. (5) can be reduced step by step as

$$\overline{\mathrm{DLI}_0}\left(x_\mathrm{c},\tau\right)=-\int_{x_c-\tau/2}^{x_c+\tau/2} f_\mathrm{ve}\left(x\right)\cdot w\left(x\right)\mathrm{d}x+EI\cdot\mathrm{BC}\left(x_c,\tau\right) \tag{6}$$

in which,

$$f_\mathrm{ve}\left(x\right)=EI\frac{\mathrm{d}^4\eta\left(x-x_c\right)}{\mathrm{d}x^4}-\rho S\omega^2\cdot\eta\left(x-x_c\right) \tag{7}$$

$$\mathrm{BC}\left(x_c,\tau\right)=\left[\sum_{i=0}^{3}\left(-1\right)^i w^{(3-i)}\left(x\right)\cdot\eta^{(i)}\left(x-x_c\right)\right]_{x_c-\tau/2}^{x_c+\tau/2} \tag{8}$$

In the above expressions, $\overline{\mathrm{DLI}_0}\left(x_\mathrm{c},\tau\right)$ is the damage location index in the interval [x_c-τ/2, x_c+τ/2] centered at position x_c with subscript ‘0’ indicating the highest derivative order of $w(x)$. It is obvious that $f_\mathrm{ve}(x)$ shares the same form as Eq. (1) by replacing the actual displacement $w(x)$ with the weight function $\eta(x)$. Therefore, $\eta(x)$ can be regarded as the virtual displacement of the VE of a length τ, having the same material properties as the real beam element. f_ve can then be regarded as the virtual force applied on the VE. BC(x_c, τ) is related to the boundary condition of the VE, which is the sum of a series of products of the actual and virtual displacements. The superscripts, (i), of $w(x)$ and $\eta(x)$ in Eq. (8) are the derivative order. The boundary part BC(x_c, τ) includes the 1st to 3rd order of derivatives of $w(x)$ in which the second order of $w(x)$ at the boundary of VE can be measured directly by strain gage [24, 25] or piezoelectric sensor [26].

In Eq. (6), the choice of $\eta(x)$ is crucial to the “weak” formulation. Since $w(x)$ and its

second order derivative can be measured by sensors directly at the VE boundary without the use of finite difference, a suitable $\eta(x)$ can eliminate unwanted derivatives terms of $w(x)$, thus enhancing the noise immunity of the detection.

3.2 Selection of the weigh function $\eta(x)$

According to the description above, the most straightforward way to remove $w^{(1)}(x)$ and $w^{(3)}(x)$ in Eq. (8) is to choose $\eta(x)$ in such a way that:

$$\left.\frac{\mathrm{d}^2\eta(x)}{\mathrm{d}x^2}\right|_{x=-\tau/2} = \left.\frac{\mathrm{d}^2\eta(x)}{\mathrm{d}x^2}\right|_{x=+\tau/2} = 0 \tag{9}$$

$$\left.\eta(x)\right|_{x=-\tau/2} = \left.\eta(x)\right|_{x=+\tau/2} = 0 \tag{10}$$

Going back to the VE, these boundary conditions state the VE can be regarded as a simply-supported beam at both ends. VE shares the same material parameters with the actual beam and the length is τ according to Eq. (7). It can be seen from Eq. (6) that it is possible to completely eliminate the integration term by letting $f_{\mathrm{ve}}(x)$ equal to zero, as

$$EI\frac{\mathrm{d}^4\eta(x-x_c)}{\mathrm{d}x^4} - \rho S\omega^2\cdot\eta(x-x_c) = 0 \tag{11}$$

Eq. (11) indicates that the virtual force $f_{\mathrm{ve}}(x)$ is zero and the solution of $\eta(x)$ is the free vibration response of the VE. Thus, by tuning the actual excitation frequency to the natural frequency of the VE, $\eta(x)$ corresponds to the mode shape of VE. For example, when the actual excitation frequency ω equals to the first natural frequency of the VE, as

$$\omega = \left(\frac{\pi}{\tau}\right)^2\sqrt{\frac{EI}{\rho S}} \tag{12}$$

$\eta(x)$ is the first mode shape of VE, expressed as

$$\eta(x) = \sin\frac{\pi}{\tau}x \tag{13}$$

Finally, Eq. (6) at these specific frequencies (any of the natural frequency of the VE) can be

simplified as

$$\overline{\mathrm{DLI}}\left(x_{\mathrm{c}},\tau\right)=\frac{\overline{\mathrm{DLI}_0}\left(x_{\mathrm{c}},\tau\right)}{EI}=\frac{\pi}{\tau}\left[\left.\frac{\mathrm{d}^2w\left(x\right)}{\mathrm{d}x^2}\right|_{x_{\mathrm{c}}-\tau/2}+\left.\frac{\mathrm{d}^2w\left(x\right)}{\mathrm{d}x^2}\right|_{x_{\mathrm{c}}+\tau/2}\right]-\frac{\pi^3}{\tau^3}\left[\left.w\left(x\right)\right|_{x_{\mathrm{c}}-\tau/2}+\left.w\left(x\right)\right|_{x_{\mathrm{c}}+\tau/2}\right] \quad (14)$$

Eq. (14) shows that the damage location index in this “weak” formulation can be readily obtained through virtual element boundary measurement (VEBM) at the natural frequency of the VE, significantly reducing the number of the measurement points. The method only requires the measurement of w and $w^{(2)}$ at VE boundaries. Hence, Eq. (14) provides a novel scheme to detect the damage in a beam component that can be implemented by several steps:

(1) Divide the entire structure into several VEs of length τ, depending on the accuracy required for locating the damage.

(2) Tune the frequency of the actual excitation to the first (or any other, in principle) natural frequency of the VE. It should be mentioned that the estimation of the parameters such as E, I, ρ and S is obviously not error free with respect to the true values. Therefore, a fast scan process based on sweeping frequency of the excitation can be carried out to accurately find the frequency ω within which the distance between the adjacent vibration nodes of the beam is equal to τ.

(3) Measure the displacement and its 2nd order derivatives at the boundary of VE. Notably, if strain gauges or piezoelectric sensors are used to measure the strains s directly, the corresponding 2nd order derivatives of the displacements can be obtained as

$$\mathrm{d}^2w\left(x\right)/\mathrm{d}x^2=2s/h \quad (15)$$

where h is the thickness of the beam. Alternatively, this second order derivative can also be obtained using a finite different scheme based on displacement measurement.

(4) Calculate the damage location index according to Eq. (14) to detect the damage location.

It is relevant to note that the VEBM based "weak" formulation can also be extended to plate component in similar way. Different from a beam component, VEs in the plate component are a series of virtual square thin-plates with the same length. The final variant of the two-dimensional "weak" formulation shares similar form as Eq. (14), given as

$$\begin{aligned}\overline{\mathrm{DLI}}(x_c, y_c, a) = &\int_{y_c-a/2}^{y_c+a/2} -\frac{\pi}{a}\sin\left(\frac{\pi}{a}y\right)\nabla^2\left[w(x_c-a/2,y)+w(x_c+a/2,y)\right]\mathrm{d}y \\ &+\int_{y_c-a/2}^{y_c+a/2}\frac{\pi^3}{a^3}\sin\left(\frac{\pi}{a}y\right)\left[w(x_c-a/2,y)+w(x_c+a/2,y)\right]\mathrm{d}y \\ &+\int_{x_c-a/2}^{x_c+a/2} -\frac{\pi}{a}\sin\left(\frac{\pi}{a}x\right)\nabla^2\left[w(x,y_c-a/2)+w(x,y_c+a/2)\right]\mathrm{d}x \\ &+\int_{x_c-a/2}^{x_c+a/2}\frac{\pi^3}{a^3}\sin\left(\frac{\pi}{a}x\right)\left[w(x,y_c-a/2)+w(x,y_c+a/2)\right]\mathrm{d}x \end{aligned} \tag{16}$$

where (x_c, y_c) and a are the center position and length of the VE, ∇^2 is the Laplacian operator that can be written as

$$\nabla^2 = \frac{\partial^2}{\partial x^2}+\frac{\partial^2}{\partial y^2} \tag{17}$$

Likewise, the two-dimensional "weak" formulation shown by Eq. (16) is derived under a steady vibration with the excitation frequency equal to the natural frequency of VE, given as

$$\omega = \frac{2\pi^2}{a^2}\sqrt{\frac{D}{\rho h}} \tag{18}$$

From Eq. (1) to Eq. (16), PE approach offers a series of variants of DLI for damage localization. In particular, the VEBM based "weak" formulation provides a

dimension-reduced measurement strategy, reducing the full field measurement to point or edge measurement in beam and plate component, respectively. Furthermore, the proposed "weak" formulation brings about significant improvement in the robustness for damage detection far beyond what the signal processing method can do, to be demonstrated in the following sections. However, compared with "strong" formulation that can identify the exact damage position, VEBM based "weak" formulation can only determine the damaged VE. In order to improve the resolution, small length τ of VE should be used, which requires a higher excitation frequency and more measurement points.

4 Validation of the VEBM based damage detection

4.1 Numerical simulations

4.1.1 Finite element (FE) model

Considering an Euler-Bernoulli cantilever beam as shown in Fig. 2, the geometrical and material parameters are listed in Table 1. Without loss of generality, a transverse surface slit, 2 mm in length and 2 mm in depth, extending uniformly along the width of the beam, is used to simulate the damage. The slit is located at x = 225 mm (Fig. 2 for the coordinate system). A FE model is created using commercial FE code ABAQUS®. In order to accurately model the slit, the beam element size is set to 1 mm, resulting in a total of 605 elements in the entire structure. A harmonic point-excitation force is applied at x = 601 mm. According to Eq. (12), the excitation frequency is set to 3180 Hz that is the 1st natural frequency of the VE which is 60 mm long.

Theoretically, the proposed method can detect damages, located anywhere inside the free surfaces. However, damage location index is different from zero at the fixed support position or load point. Therefore, the proposed method applies to the points close to the support or

excitation, but not exactly at these points. To avoid the influence from the boundary and the excitation point, an inspection region, within the interval [30, 570], is chosen. The flexural displacement w_{exact} at each element node is shown in Fig. 3(a). It should be noted that PE approach is independent of the amplitude of the excitation. So the level of the excitation can be arbitrary. To quantitatively examine the noise immunity capability of the proposed approach, the white Gaussian noise with three different energy levels, which are 10^{-7}, 10^{-5}, 10^{-3} of signal energy, are added to the exact displacement w_{exact}. The noisy displacements w_{noisy} are shown in Figs. 3(b-d).

4.1.2 Results and discussions

Using "strong" formulation stated in Eq. (4), the constructed DLI_{exact} and DLI_{noisy} that correspond to the exact displacement w_{exact} and the noisy displacements w_{noisy} are shown in Figs. 4(a-d), respectively. Using 541 measurement points, Fig. 4(a) indicates the damage location explicitly where DLI_{exact} reaches the peak value whilst dowelling around zero in the pristine region. On the contrary, Figs. 4(b-d) show that the resolution of damage detection reduces as the noise level increases. For 10^{-5} and 10^{-3} cases, DLI_{noisy} fail to detect the damage location, due to the venerable noise immunity capacity. In fact, the 4th order derivative over the measured displacement w_{noisy} overwhelms and completely masks the damage-induced peak in DLI_{noisy}, in agreement with the previous analyses.

Using the proposed VEBM approach, the entire structure is divided into nine elements of the same length by ten measurement points as shown in Fig. 5. Each VE is 60 mm long, which is the distance between each two adjacent measurement points. An excitation frequency of 3180 Hz, corresponding to the first natural frequency of the VEs, is used to excite the structure. Based on Eq. (14), both w and its 2nd order derivative $w^{(2)}$ are required. In the

present case, $w^{(2)}$ at the i-th measurement point is obtained by mean of finite difference as

$$w_i^{(2)} = \frac{w_{i+1} - 2w_i + w_{i-1}}{d_{\mathrm{m}}^2} \tag{19}$$

where two points, adjacent to i-th measurement point are used. Compared with the "strong" formulation, VEBM based "weak" formulation only uses 30 measurement points in the inspection region [30, 570]. $\overline{\mathrm{DLI}}_{\mathrm{extact}}$ and $\overline{\mathrm{DLI}}_{\mathrm{noisy}}$ are then calculated by Eq. (14) using w_{exact} and w_{noisy}, respectively. Placing $\overline{\mathrm{DLI}}$ to the corresponding position of each VE, detection results are given in Figs. 5(a-d), respectively. It can be seen that all figures show the corresponding damaged VE with a high damage location index value. To quantify the detection results, a DNR (damage location index-to-noise ratio) in dB is defined as

$$\mathrm{DNR} = 10\log\frac{\overline{\mathrm{DLI}}(\mathrm{damage})}{\overline{\mathrm{DLI}}(\mathrm{healthy})} \tag{20}$$

where $\overline{\mathrm{DLI}}(\mathrm{damage})$ and $\overline{\mathrm{DLI}}(\mathrm{healthy})$ are the average values of the damage location indices in the actual damage region and healthy region, respectively. Similar as the commonly used signal-to-noise ratio (SNR) in signal processing, DNR is a measure to evaluate the level of a desired detection result compared with the level of background noise. The detection results using "strong" formulation and VEBM approach with different noise levels are listed in Table 2. Obviously, the effect of the added noise can be clearly observed from DNR reduction with the increasing noise level. Nevertheless, the beam segment containing the damage can still be accurately detected by VEBM approach even with a high DNR. Compared with "strong" formulation, VEBM approach shows an enhanced noise immunity capacity.

It is relevant to mention that the error caused by the finite difference is still unavoidable due to the use of Eq. (19). Using w_{exact} and w_{noisy} with the noise energy 10^{-3}, the 1st to 4th

order derivatives of w as well as their discrepancies from the true values are calculated (calculated difference between the results with and without the noise). The root mean square (RMS) of the discrepancies, expressed in dB, is shown in Fig. 6, showing an increasing noise effect when the order of derivative increases. Alternatively, $w_i^{(2)}$ can also be directly obtained by measuring the strain at the two boundary points of the VE. This will avoid indirect calculation of the $w_i^{(2)}$ through finite difference scheme and, by the same token, further reduce the noise effect and measurement points at the same time.

Compared with Eq. (4), the VEBM based "weak" formulation that is defined by Eq. (14) seems to be independent on the material parameters such as E, I, ρ and S. However, this benefit does not come without price. In fact, Eq. (14) can be regarded as a special case of Eq. (4) that is only applicable to the natural frequency of the VE. To choose the suitable excitation frequency, the material parameters are implicitly required. Therefore, discrepancies between the excitation frequency and the estimated natural frequency of VE are unavoidable. To investigate this problem and its influence on the detection accuracy in practical implementation, the excitation frequency is artificially set to have a variation margin of plus or minus 50 Hz in the FE model. On the other hand, the obtained displacements are still processed with the VEBM based "weak" formulation to construct $\overline{\mathrm{DLI}}$ by using Eq. (14). The distributions of $\overline{\mathrm{DLI}}$ are shown in Figs. 7(a) and (b). DNR results using different excitation frequencies are tabulated in Table 3. It can be seen that the damage can still be detected within a certain frequency range around the accurate natural frequency of the VE, although the VEBM based "weak" formulation requires that the excitation frequency be the natural frequency of VE strictly. However, the accuracy of the detection results decreases when the excitation frequency shifts further away from the natural frequency of VE as shown in Table 3.

4.2 Experimental verifications

4.2.1 Experimental setup

Experimental verification was subsequently conducted using a cantilever beam containing an artificial damage, which is a rectangular slit (2×2 mm) extending along the width of the beam. The beam, made of aluminum 6061, was fixed-supported on a testing table (NEWPORT® ST-UT2), as shown in Fig. 8. The detailed dimensions and the material parameters of the structure were the same as those used in the FE model, listed in Table 1 and shown in Fig. 2. Through a power amplifier (B&K® 2718), an electromechanical shaker (B&K® 4809) was used to provide a harmonic point-force excitation to the structure at x = 601 mm. A scanning Laser Doppler Vibrometer (Polytec® PSV-400B) was used to measure the out-of-plane displacement of the beam, within the selected inspection region from x = 30 mm to x = 570 mm. The natural frequency of the VE was estimated to be 3180 Hz by Eq. (12), at which the steady-state vibration response was measured, with results shown in Fig. 9.

4.2.2 PE approach using "strong" formulation

For comparison, the "strong" formulation was firstly applied. According to Fig. 9, the measured displacement under laboratory condition shows a high SNR that makes it possible to detect the damage using "strong" formulation. Using a 2.3 mm interval, 235 measurement points were used to construct the DLI according to Eq. (4). Fig. 10(a) shows that the DLI such constructed fails to delineate the damage position, because of the measurement noise magnified by the high order derivative. However, by increasing the interval to 3.5 mm, corresponding to 158 measurement points, an obvious improvement is observed, as shown in Fig. 10(b), in agreement with the optimal measurement density criterion suggested by the previous work [16]. The optimal interval between two measurement points balances the

accuracy of the finite difference calculation and the noise immunity. According to Eq. (20), the corresponding DNR is 6.6 dB.

4.2.3 PE approach using VEBM based "weak" formulation

Using nine VEs, 60mm in length, reducing the measurement points from 158 to 30, the displacement of the measurement points and their second order derivatives at the virtual element boundaries are obtained. Fig. 11 shows the damage location index by using Eq. (14). The significant peak value can be clearly observed at the damaged VE position. Characterized by DNR, VEBM based "weak" formulation not only reduces the measurement points, but also improves the detection accuracy from 6.6 dB in the "strong" formulation to 7.4 dB.

5 Conclusions

In spite of many appealing features of the Pseudo-Excitation (PE) approach, the "strong" formulation approach is shown to be highly sensitive to measurement noise and requires a large amount of measurement points within the inspection region. To tackle the problem, this paper presents a new "weak" formulation based on Virtual Element Boundary Measurement (VEBM). The proposed method, along with the mathematical framework, establishes a new paradigm for PE-based damage detection, shifting the "point-to-point" detection modality of the strong formulation to "region-by-region" detection philosophy. The VEBM based "weak" formulation segments the entire structure into a series of so-called "virtual elements" (VE). By tuning the excitation frequency to the natural frequency of the VE, the VEBM based "weak" formulation allows eliminating higher order derivative over the structural displacement, which is mainly responsible for the deficiency of the "strong formulation" in detecting structural damages in the presence of the measurement noise. By the same token, the proposed VEBM based "weak" formulation only requires a small number of measurement

points at the virtual element boundaries. Through numerical examples, it is also shown that the proposed method is able to tolerate variations of the excitation frequencies to a certain extent as a result of inaccurate estimation of the structural physical parameters. Both numerical and experimental studies show that the VEBM based approach is able to achieve satisfactory detection results by using a small number of measurement points, whilst providing enhanced noise immunity capability against measurement noise and uncertainties.

It is relevant to note that the VEBM based "weak" formulation only requires the displacements and its second order derivatives to be estimated at the boundaries of VEs. The latter can also be readily measured by strain gauge or piezoelectric sensors. This will avoid calculating the second order derivatives of structure displacement, thus further reducing the number of measurement points and increasing the robustness of the method at the same time.

Acknowledgments

This work was supported partially by the National Natural Science Foundations of China (No. 11272272). Authors wish to acknowledge the support given to them by the Hong Kong Polytechnic University (Research Grant G-YK14) and the NUAA State Key Laboratory Program under Grant MCMS-0514K01. The first author acknowledges the funding of Jiangsu Innovation Program for Graduate Education (CXZZ13_0157) and the Fundamental Research Funds for the Central Universities.

References

[1] B.W. Drinkwater, P.D. Wilcox, Ultrasonic arrays for non-destructive evaluation: A review, NDT & E International, 39 (2006) 525-541.

[2] J. Cheng, H. Ji, J. Qiu, T. Takagi, T. Uchimoto, N. Hu, Novel electromagnetic modeling approach of carbon fiber-reinforced polymer laminate for calculation of eddy currents and

eddy current testing signals, Journal of Composite Materials, (2014) 0021998314521475.

[3] W. Ren, J. Liu, G.Y. Tian, B. Gao, L. Cheng, H. Yang, Quantitative non-destructive evaluation method for impact damage using eddy current pulsed thermography, Composites Part B: Engineering, 54 (2013) 169-179.

[4] C. Zhang, J. Qiu, H. Ji, Laser Ultrasonic Imaging for Impact Damage Visualization in Composite Structure, in: EWSHM-7th European Workshop on Structural Health Monitoring, 2014.

[5] J. Chen, Z. Su, L. Cheng, Identification of corrosion damage in submerged structures using fundamental anti-symmetric Lamb waves, Smart Materials and Structures, 19 (2010) 015004.

[6] M. Yoon, D. Heider, J. Gillespie Jr, C. Ratcliffe, R. Crane, Local damage detection using the two-dimensional gapped smoothing method, Journal of Sound and Vibration, 279 (2005) 119-139.

[7] U. Baneen, N. Kinkaid, J. Guivant, I. Herszberg, Vibration based damage detection of a beam-type structure using noise suppression method, Journal of Sound and Vibration, 331 (2012) 1777-1788.

[8] W. Fan, P. Qiao, Vibration-based damage identification methods: a review and comparative study, Structural Health Monitoring, 10 (2011) 83-111.

[9] J.-T. Kim, Y.-S. Ryu, H.-M. Cho, N. Stubbs, Damage identification in beam-type structures: frequency-based method vs mode-shape-based method, Engineering structures, 25 (2003) 57-67.

[10] Y. Yan, L. Cheng, Z. Wu, L. Yam, Development in vibration-based structural damage detection technique, Mechanical Systems and Signal Processing, 21 (2007) 2198-2211.

[11] M. Benedetti, V. Fontanari, D. Zonta, Structural health monitoring of wind towers: remote damage detection using strain sensors, Smart Materials and Structures, 20 (2011)

055009.

[12] M. Radzieński, M. Krawczuk, M. Palacz, Improvement of damage detection methods based on experimental modal parameters, Mechanical Systems and Signal Processing, 25 (2011) 2169-2190.

[13] A. Tomaszewska, Influence of statistical errors on damage detection based on structural flexibility and mode shape curvature, Computers & structures, 88 (2010) 154-164.

[14] M. Rucka, K. Wilde, Application of continuous wavelet transform in vibration based damage detection method for beams and plates, Journal of Sound and Vibration, 297 (2006) 536-550.

[15] S. Na, H. Lee, A technique for improving the damage detection ability of the electro-mechanical impedance method on concrete structures, Smart Materials and Structures, 21 (2012) 085024.

[16] H. Xu, L. Cheng, Z. Su, J.-L. Guyader, Identification of structural damage based on locally perturbed dynamic equilibrium with an application to beam component, Journal of Sound and Vibration, 330 (2011) 5963-5981.

[17] M. Cao, L. Cheng, Z. Su, H. Xu, A multi-scale pseudo-force model in wavelet domain for identification of damage in structural components, Mechanical Systems and Signal Processing, 28 (2012) 638-659.

[18] H. Xu, L. Cheng, Z. Su, J.-L. Guyader, Damage visualization based on local dynamic perturbation: Theory and application to characterization of multi-damage in a plane structure, Journal of Sound and Vibration, 332 (2013) 3438-3462.

[19] H. Xu, Z. Su, L. Cheng, J.-L. Guyader, P. Hamelin, Reconstructing interfacial force distribution for identification of multi-debonding in steel-reinforced concrete structures using noncontact laser vibrometry, Structural Health Monitoring, 12 (2013) 507-521.

[20] H. Xu, Z. Su, L. Cheng, J. Guyader, A "Pseudo-excitation" approach for structural

damage identification: From "Strong" to "Weak" modality, Journal of Sound and Vibration, 337 (2015) 181-198.

[21] C. Pezerat, J.L. Guyader, Identification of vibration sources, Applied Acoustics, 61 (2000) 309–324.

[22] S. Chesne, J.L. Guyader, C. Pezerat, Identification of Plate Boundary Forces From Measured Displacements, Journal of Vibration & Acoustics, 130 (2008) 1257-1261.

[23] A. Berry, O. Robin, F. Pierron, Identification of dynamic loading on a bending plate using the virtual fields method, Journal of Sound & Vibration, 333 (2014) 7151–7164.

[24] E.-T. Lee, S. Rahmatalla, H.-C. Eun, Damage detection by mixed measurements using accelerometers and strain gages, Smart Materials and Structures, 22 (2013) 075014.

[25] Y. Li, L. Cheng, L. Yam, W. Wong, Identification of damage locations for plate-like structures using damage sensitive indices: strain modal approach, Computers & structures, 80 (2002) 1881-1894.

[26] C. Zhang, J. Qiu, H. Ji, S. Shan, An imaging method for impact localization using metal-core piezoelectric fiber rosettes, Journal of Intelligent Material Systems and Structures, (2014) 1045389X14551432.

Table and Figure Captions

Table 1. Geometrical and material parameters of the cantilever beam.

Table 2. DNRs of the detection results with different noise levels.

Table 3. DNRs of the detection results using different excitation frequencies.

Fig. 1. A typical complex structure with dynamic responses satisfying local equation of motion on various structural components.

Fig. 2. A cantilever beam with an artificial damage.

Fig. 3. Displacements using FE simulation (a) without noise; and (b-d) with different levels of white Gauss noise (the noise is 10^{-7}, 10^{-5}, 10^{-3} of signal energy)

Fig. 4. Magnitude of DLI by "strong" formulation using (a) w_{exact}; and (b-d) w_{noisy} with different noise levels (the noise is 10^{-7}, 10^{-5}, 10^{-3} of signal energy).

Fig. 5. Magnitude of $\overline{\text{DLI}}$ by VEBM based "weak" formulation using (a) w_{exact}; and (b-d) w_{noisy} with different noise levels (the noise is 10^{-7}, 10^{-5}, 10^{-3} of signal energy).

Fig. 6. Noise level in the different orders of displacement derivatives with Gauss noise (the noise in displacement is 1‰ of signal energy).

Fig. 7. Magnitude of $\overline{\text{DLI}}$ by VEBM based "weak" formulation with different excitation frequencies (a) 3130 Hz; and (b) 3230 Hz, when accurate natural frequency of VE is 3180 Hz.

Fig. 8. Test-rig and experimental setup.

Fig. 9. Steady-state vibration displacement $w(x)$ captured experimentally.

Fig. 10. Magnitude of DLI by "strong" formulation with the measurement interval (a) 2.3 mm and (b) 3.5 mm.

Fig. 11. Magnitude of $\overline{\text{DLI}}$ by VEBM based "weak" formulation using experimental data.

Tables

Table 1

Geometrical and material parameters of the cantilever beam.

Beam width b [mm]	36
Beam thickness h [mm]	5
Beam length l [mm]	605
Damage length l_d [mm]	2
Damage depth h_d [mm]	2
Density ρ [kg/m^3]	2700
Elastic modulus E [GPa]	68.9

Table 2

DNRs of the detection results with different noise levels.

Noise energy level	DNR (Strong formulation)	DNR (VEBM approach)
10^{-7}	15.69 dB	13.97 dB
10^{-5}	3.70 dB	13.86 dB
10^{-3}	-0.42 dB	9.83 dB

Table 3

DNRs of the detection results using different excitation frequencies.

Frequency	DNR
3130 Hz	12.82 dB
3180 Hz (natural frequency of VE)	14.25 dB
3230 Hz	10.03 dB

Figures

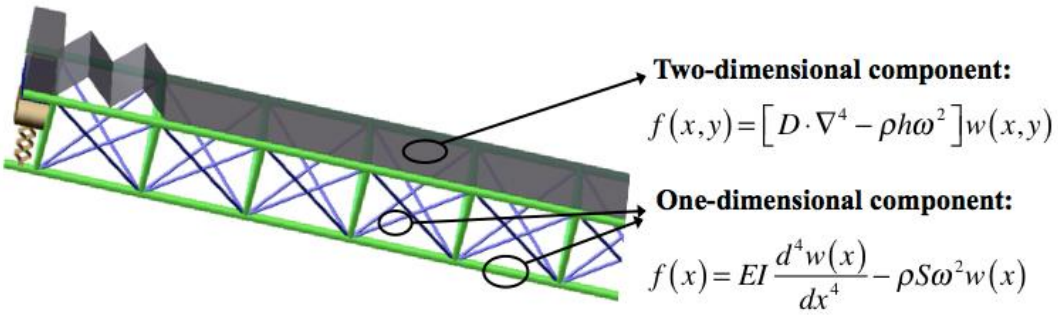

Fig. 1. A typical complex structure with dynamic responses satisfying local equation of motion on various structural components.

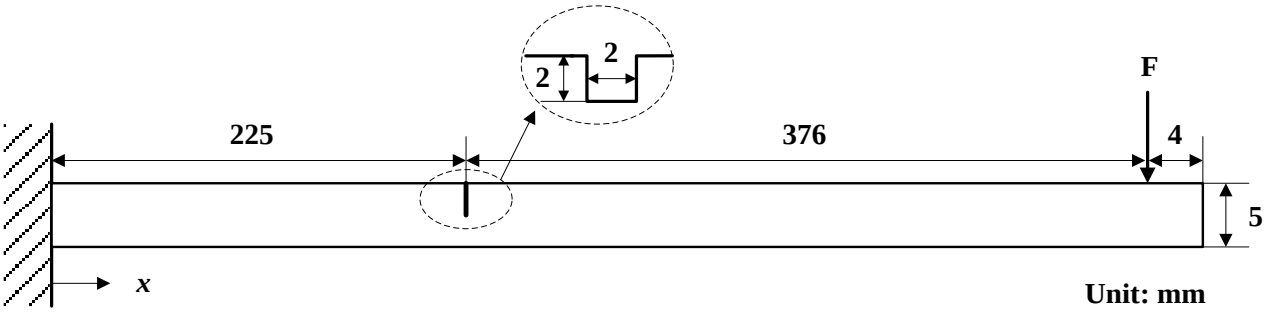

Fig. 2. A cantilever beam with an artificial damage.

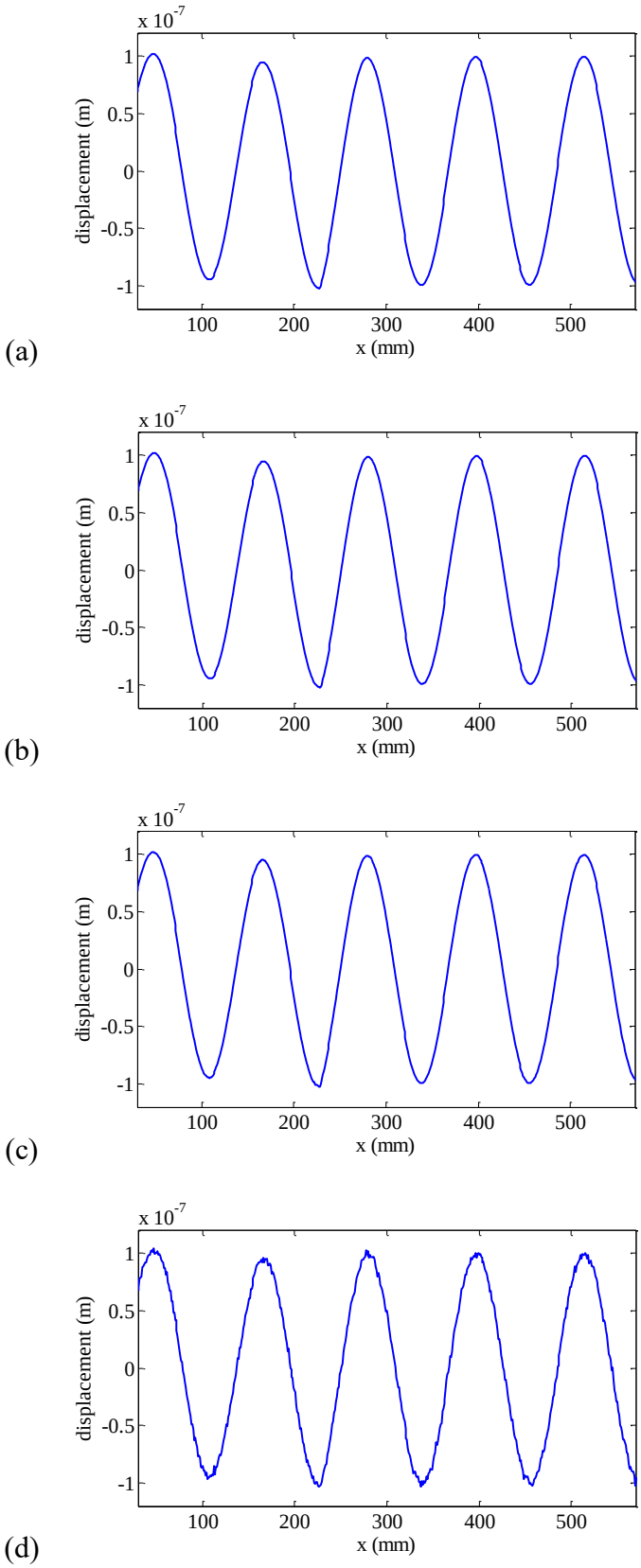

Fig. 3. Displacements using FE simulation (a) without noise; and (b-d) with different levels of white Gauss noise (the noise is 10^{-7}, 10^{-5}, 10^{-3} of signal energy).

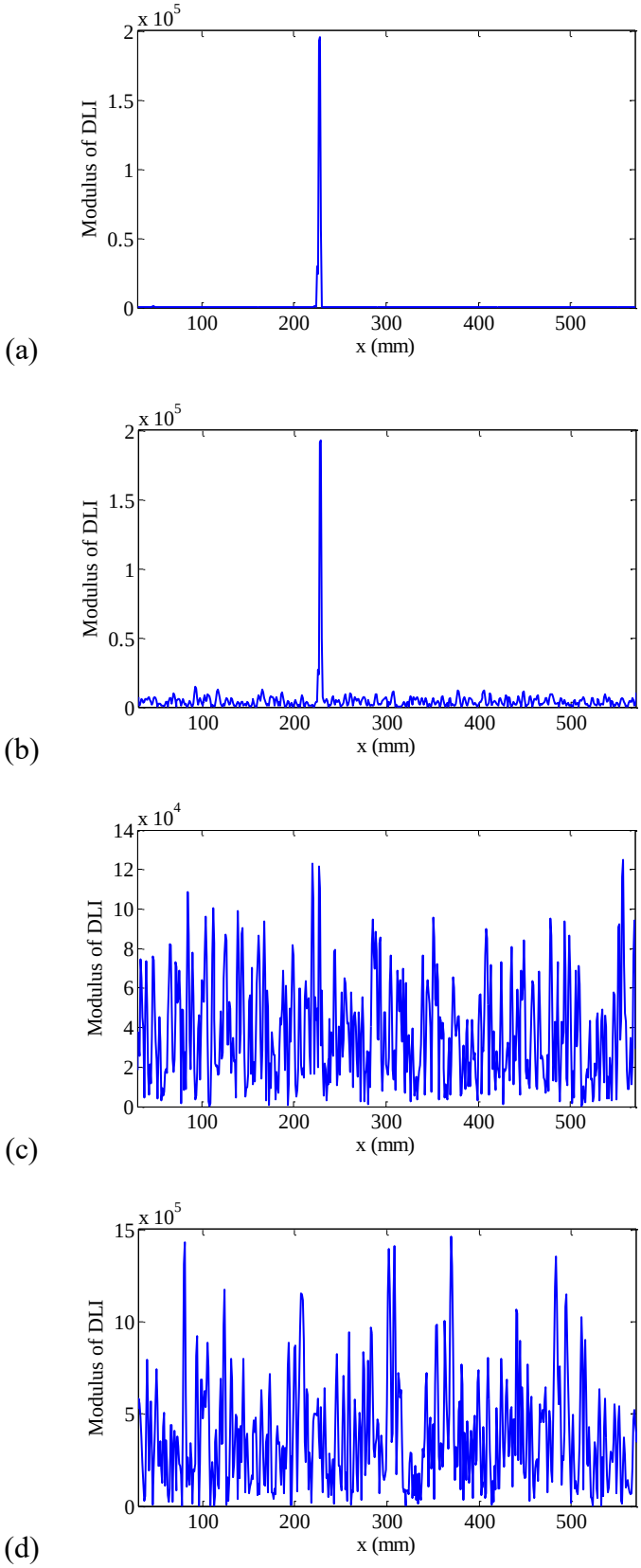

Fig. 4. Magnitude of DLI by "strong" formulation using (a) w_{exact}; and (b-d) w_{noisy} with different noise levels (the noise is 10^{-7}, 10^{-5}, 10^{-3} of signal energy).

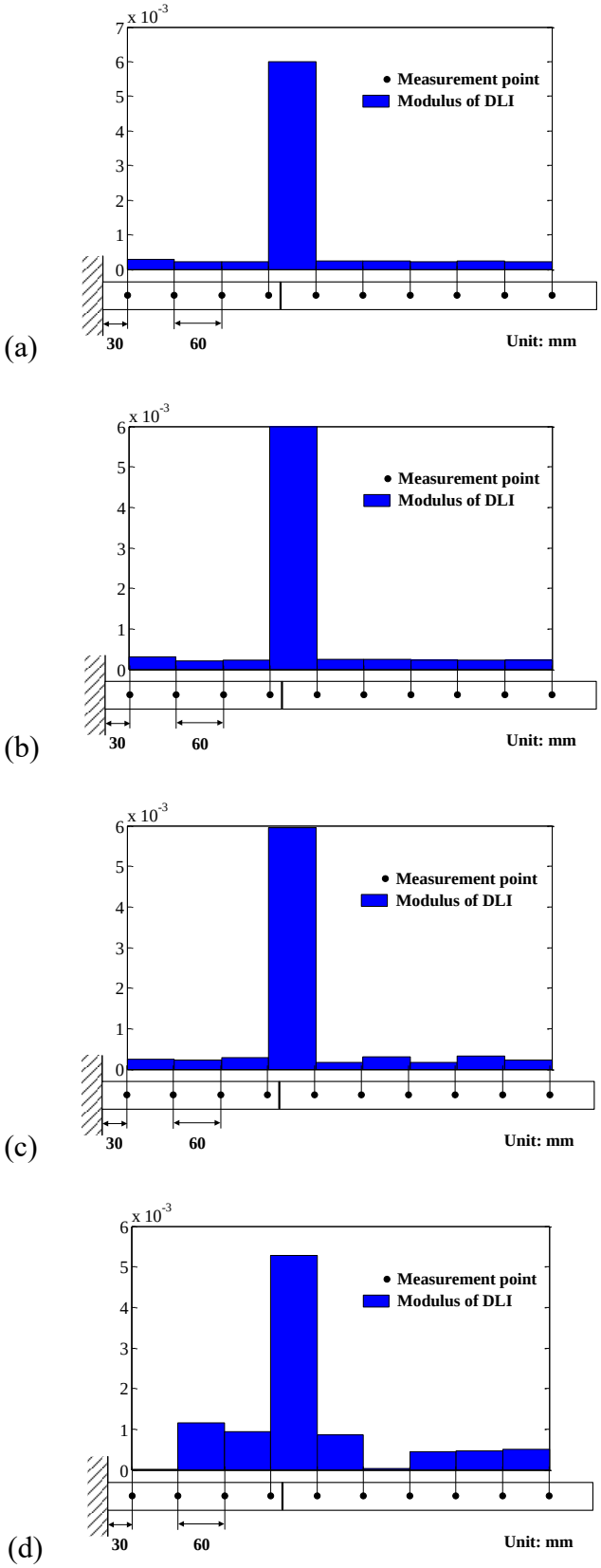

Fig. 5. Magnitude of $\overline{\mathrm{DLI}}$ by VEBM based "weak" formulation using (a) w_{exact}; and (b-d) w_{noisy} with different noise levels (the noise is 10^{-7}, 10^{-5}, 10^{-3} of signal energy).

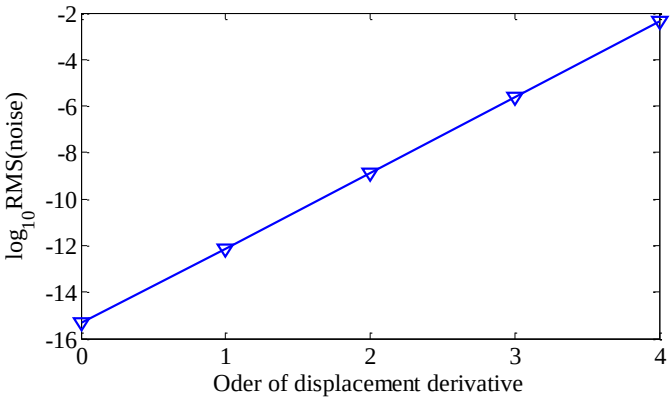

Fig. 6. Noise level in the different orders of displacement derivatives with Gauss noise (the noise in displacement is 1‰ of signal energy).

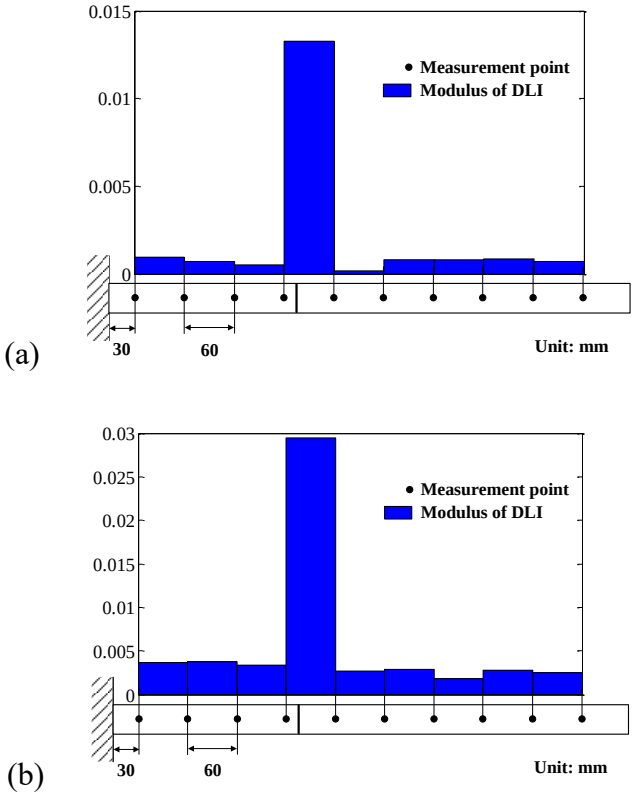

Fig. 7. Magnitude of $\overline{\mathrm{DLI}}$ by VEBM based "weak" formulation with different excitation frequencies (a) 3130 Hz; and (b) 3230 Hz, when accurate natural frequency of VE is 3180 Hz.

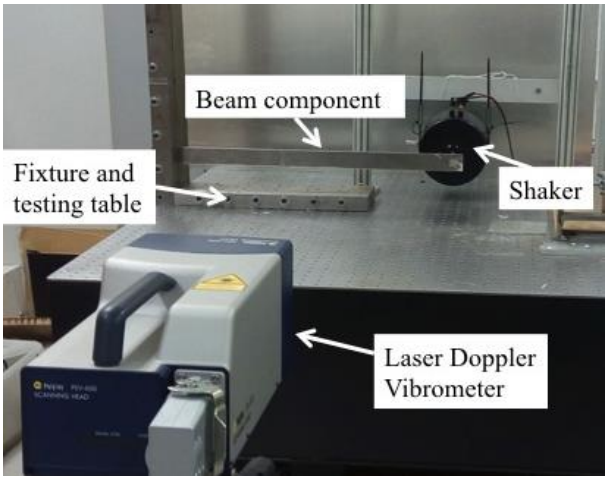

Fig. 8. Test-rig and experimental setup.

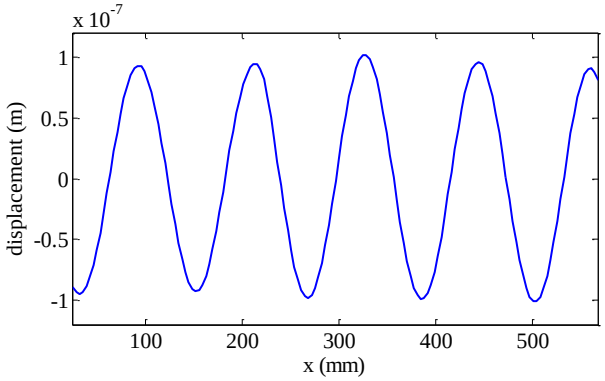

Fig. 9. Steady-state vibration displacement $w(x)$ captured experimentally.

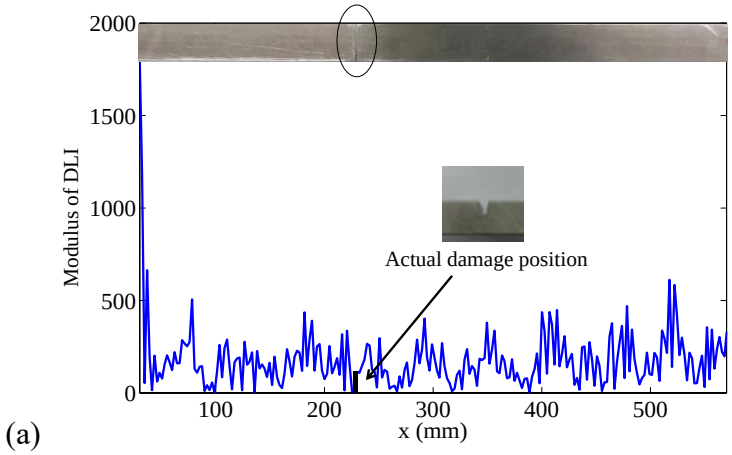

(a)

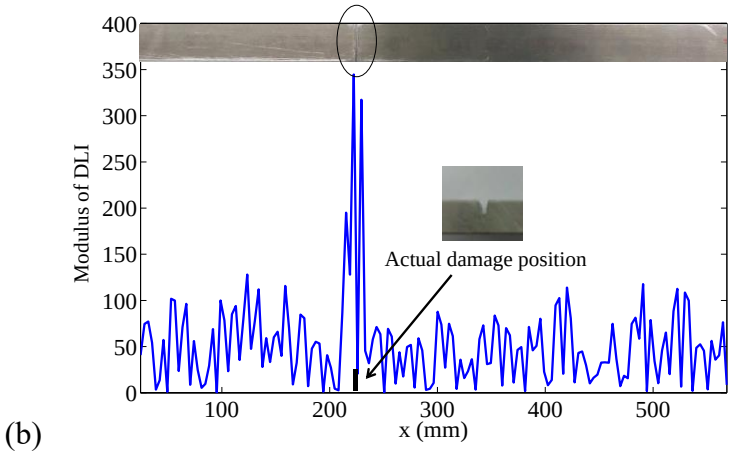

(b)

Fig. 10. Magnitude of DLI by "strong" formulation with the measurement interval (a) 2.3 mm and (b) 3.5 mm.

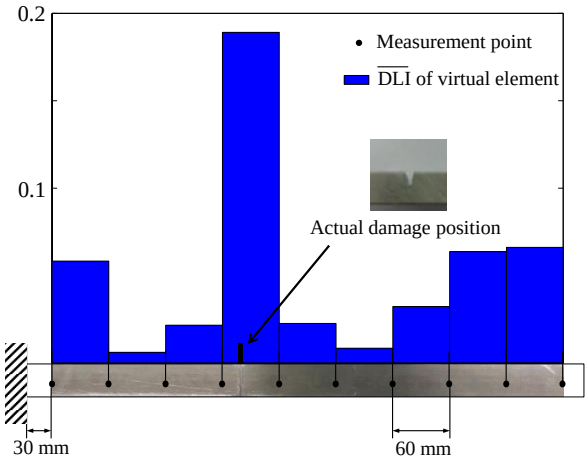

Fig. 11. Modulus of $\overline{\text{DLI}}$ by VEBM based "weak" formulation using experimental data.